Immunogenetics (2019) 71:489–499
https://doi.org/10.1007/s00251-019-01124-x

ORIGINAL ARTICLE

Methylation of H3K27 and H3K4 in key gene promoter regions of thymus in RA mice is involved in the abnormal development and differentiation of iNKT cells

Ming Meng[1,2] · Huifang Liu[1,2] · Shengde Chen[1,2] · Huijuan Zhao[1,2] · Xiang Gao[1,2] · Jingnan Zhang[1,2] · Dongzhi Chen[1,2,3]

Received: 13 April 2019 / Accepted: 19 June 2019 / Published online: 11 July 2019

Abstract

Epigenetic modifications have been shown to be important for immune cell differentiation by regulating gene transcription. However, the role and mechanism of histone methylation in the development and differentiation of iNKT cells in rheumatoid arthritis (RA) mice have yet to be deciphered. The DBA/1 mouse RA model was established by using a modified GPI mixed peptide. We demonstrated that total peripheral blood, thymus, and spleen iNKT cells in RA mice decreased significantly, while iNKT1 in the thymus and spleen was increased significantly. PLZF protein and PLZF mRNA levels were significantly decreased in thymus DP T cells, while T-bet protein and mRNA were significantly increased in thymus iNKT cells. We found a marked accumulation in H3K27me3 around the promoter regions of the signature gene Zbtb16 in RA mice thymus DP T cells, and an accumulation of H3K4me3 around the promoters of the Tbx21 gene in iNKT cells. The expression levels of UTX in the thymus of RA mice were significantly reduced. The changes in the above indicators were particularly significant in the progressive phase of inflammation (11 days after modeling) and the peak phase of inflammation (14 days after modeling) in RA mice. Developmental and differentiation defects of iNKT cells in RA mice were associated with abnormal methylation levels (H3K27me3 and H3K4me3) in the promoters of key genes Zbtb16 (encoding PLZF) and Tbx21 (encoding T-bet). Decreased UTX of thymus histone demethylase levels resulted in the accumulation of H3K27me3 modification.

Keywords RA · iNKT · Epigenetic · UTX · H3K27me3 · H3K4me3

Highlights
- The decrease of iNKT cells and the imbalance of subsets in RA are related to the abnormal development and differentiation of iNKT.
- Developmental and differentiation defects of iNKT cells in RA mice were associated with abnormal methylation levels of key genes Zbtb16 and Tbx21 promoters H3K27me3 and H3K4me3.
- Decreased UTX of thymus histone demethylase resulted in the accumulation of H3K27me3 modification.

✉ Dongzhi Chen
chenddzz@163.com

[1] Medical School of Hebei University, Baoding, People's Republic of China

[2] Key Laboratory of Pathogenesis mechanism and control of inflammatory-autoimmune diseases in Hebei Province, Baoding, People's Republic of China

[3] Department of Immunology, School of Medicine, Hebei University, Baoding, Hebei Province, People's Republic of China

Introduction

Rheumatoid arthritis (RA) is a complex chronic inflammatory autoimmune disease. The key pathogenesis of RA is immune imbalance and excessive inflammatory response (Boissier et al. 2008). In recent years, it has been found that invariant nature killer T (iNKT) cells play an important role in the development of RA. The majority of RA patients suffer from reduced numbers and abnormal function of iNKT cells (Tudhope et al. 2010; Meng et al. 2015; Véronique et al. 2010). In our previous study, we also observed a significant decrease in the number of peripheral blood iNKT cells and a reduction in their proliferation ability in the majority of RA patients (Meng et al. 2015). The modified GPI mixed peptides were used to establish the rheumatoid arthritis (RA) mouse model in this study. We found that the rates of iNKT cells in the peripheral blood, thymus, and spleen were significantly decreased,

while iNKT1 in the thymus and spleen was significantly increased (Zhang et al. 2016; Chen et al. 2019). It was suggested that the abnormal development and differentiation of iNKT in the thymus may be involved in RA.

Histone methylation has been a hot topic in the field of epigenetics (Couture and Trievel 2006; Zhang et al. 2011). The methylation modification levels of H3K27 and H3K4 in specific gene promoter regions are markers of gene activity (Bartova et al. 2008; Wang et al. 2010). Currently, it is believed that methylation of H3K27 is a marker of gene inhibition and methylation of H3K4 is a marker for gene activation (Ng et al. 2009; Yi et al. 2019). H3K27me3 histone demethylase UTX promotes target gene transcription by demethylating H3K27me3. In addition, UTX is a member of the H3K4 methyltransferase complex MLL2, which promotes gene transcription by regulating H3K4 methylation (Issaeva et al. 2007; Cho et al. 2007). PLZF is a transcription factor that regulates the early differentiation and development of thymic iNKT cells (Seiler et al. 2012; Savage et al. 2008), while the transcription factor T-bet is crucial for the terminal maturation of iNKT cells (Matsuda et al. 2006; Yue et al. 2010). To date, the epigenetic regulation of genes related to iNKT cells in RA has not been reported. In this study, UTX expression and methylation levels of H3K27 and H3K4 in thymic PLZF (Zbtb16) and T-bet (Tbx21) gene promoter regions were analyzed to investigate the epigenetic mechanism of decreased number of thymic iNKT cells and increased iNKT1 in RA. Our results provide a mechanism for the pathogenesis of RA and a potential intervention target for the treatment of RA.

Materials and methods

Experimental animals

DBA/1 mice (20.0 ± 1.0 g) were provided by Beijing Vital River Laboratory Animal Technology Co., Ltd. (License No. SCXK (Beijing) 2016-0006). The mice were maintained under specific pathogen-free conditions in the animal facility at Animal Lab of Medical Experiment Center, Hebei University, and all experiments were approved by the Animal Welfare and Ethical Committee of Hebei University (approval number IACUC-2017009).

Reagents and instruments

The hGPI325-339 and hGPI469-483 were purchased from Beijing SBS Genetech Co., Ltd. Pertussis toxin and Complete Freund's Adjuvant (CFA) were from Sigma. Eosin, hematoxylin, and Tap Water/Bluing were obtained from Hibio Technology Co., Ltd. PE-T-selected-CD1d tetramer was from MBL International Woburn MA. FITC-anti-mouse TCR-β, Percp-Cy™5.5 mouse anti-T-bet, Alexa Fluor 647 mouse anti-PLZF, and PerCP-Cy™5.5 mouse anti-ROR-ϒt were from Becton Dickinson. Foxp3/Transcription Factor Staining Buffer was purchased from eBioscience, and α-GalCer was from ENZO Life Sciences. Anti-Plzf, Anti-Tbx21, and Anti-UTX antibody were obtained from Abcam. Affinity Purified Antibody To Mouse IgG(H + L) and Affinity Purified Antibody To Rabbit IgG(H + L) were from KPL. FastKing RT Kit (With gDNase) and SuperReal PreMixPlus (SYBR Green) were purchased from Tiangen Biotech (Beijing) CO., LTO. EZ-ChIP™ was purchased from MILLIPORE. H3K4me3 (Tri-methyl Lys4) was from GeneTex. H3K27me3 (Tri-methyl Lys27) was obtained from Arigo. AnLightCycler®96 (Roche) and an Accuri C6 flow cytometer (BD) were used as well.

Grouping and establishment of the mouse RA model

A total of 10 mice were randomly selected as the healthy control group, and 30 animals were subjected to artificial modeling by administration of mixed polypeptide fragments hGPI325-339 and hGPI469-483 as follows. The polypeptide fragments were mixed and dissolved in pre-cooled triple distilled water (50 μg of mixed peptide in 75 μl water), blended with the same volume of CFA to complete emulsification, and then injected into the mouse tail root subcutaneously (150 μl per mouse); the same day and 48 h later, intraperitoneal injection of Pertussis toxin (200 ng each) was performed to boost immune reactions. Then, the RA model group was divided into three groups according to the arthritis index score, joint redness and swelling, paw thickness, and serum cytokine level of the mice, including the progressive phase of inflammation (10 mice, 11 days after modeling), the peak phase of inflammation (10 mice, 14 days after modeling), and the remission phase of inflammation (10 mice, 20 days after modeling) (Chen et al. 2019).

FCM was used to detect the rates of peripheral blood iNKT cells

Whole blood (about 120 μl per mouse) was added to a flow-cytometry tube, followed by blocking with BSA. Then, 2 μl of each of FITC-labeled anti-CD4 and PE labeled α-GalCer-loaded CD1d tetramer were added in the dark for 20 min. Next, 1 ml of erythrocyte lytic fluid was added for 8 min away from light; after centrifugation at 1000 rpm for 5 min, the supernatant was discarded and the pellet was washed with PBS twice. Finally, the cells were resuspended in 500 μl PBS and assessed by flow cytometry (Accuri C6); the CFlow software (BD) was used for data analysis.

Measurements of thymus and spleen iNKT cell rates and absolute number of thymus iNKT

The obtained thymocytes and spleen lymphocytes were placed in different flow tubes (1×10^6 cells/tube). Then, FITC labeled anti-TCR β (2 μl) and PE-labeled α-GalCer-loaded CD1d tetramers (2 μl) were incubated in 500 μl PBS reaction systems for 30 min in the dark, washed twice with PBS, and resuspended in 500 μl PBS for FACS detection. The absolute amounts of iNKT cells in the thymus were obtained by multiplying the total number of thymus cells by the rates of iNKT cells.

Subsets of thymus and spleen iNKT cells were detected by FCM

Two tubules of thymocytes (1×10^6cells/tube) and two tubules of spleen lymphocytes (1×10^6cells/tube) are described in "Measurements of thymus and spleen iNKT cell rates and absolute number of thymus iNKT" each tube after incubation with anti-TCR β and PE labeled α-GalCer-loaded CD1d tetramer for extracellular markers; the cells were permeabilized and fixed according to the specific procedure of Foxp3/Transcription Factor Staining Buffer. Then, one tube added 5 μl each of PerCPCy™5.5 mouse anti-T-bet and Alexa Fluor®647mouse anti-PLZF, another added 5 μl each of PerCPCy™5.5 mouse anti-ROR-ϒt and Alexa Fluor® 647 mouse anti-PLZF at room temperature in the dark for at least 30 min. After two washes with PBS, the cells were resuspended in 500 μl PBS and assessed by FACS.

Western blot analysis for UTX, PLZF, and T-bet

Lymphocytes, DP T cells, and iNKT cells were isolated from mouse thymus. Total cell protein was extracted and then quantitated using the Bradford method. Forty-five-microgram protein was used for gel electrophoresis and subsequent western blot analysis. After incubation with primary and secondary antibodies, protein expression levels of PLZF, T-bet, and UTX were detected using chemiluminescence. The ImageJ software was used for quantitation (gray scale values); GAPDH was used as an internal reference.

qRT-PCR for the measurement of PLZF and T-bet mRNA levels

Total RNA was extracted from cells and then quantitated using mySPEC ultraviolet-visible spectrophotometer. cDNA was synthesized using a cDNA synthesis kit. qRT-PCR was performed using SYBR green master mix on the LightCycler®96 RT-PCR detection system. β-Actin was used as the housekeeping control. The $2^{-\Delta\Delta CT}$ cycle threshold method was used to calculate relative fold change. The following primer sequences were used:

β-actin, forward, 5′-GGCTGTATTCCCCTCCATCG-3′
β-actin, reverse, 5′-CCAGTTGGTAACAATGCCATGT-3′
Zbtb16, forward, 5′-CTGGGACTTTGTGCGATGTG-3′
Zbtb16, reverse, 5′-CGGTGGAAGAGGATCTCAAACA-3′
Tbx21, forward, 5′-AGCAAGGACGGCGAATGTT-3′
Tbx21, reverse, 5′-GGGTGGACATATAAGCGGTTC-3′

ChIP-PCR for H3K27me3 and H3K4me3 determination

ChIP was performed as described with instructions. Briefly, MACS-sorted DP cells and 5×10^6 MACS-sorted iNKT cells were respectively fixed with 1% formaldehyde (EMS) for 5 min at 25 °C. The cross-linked DNA was sheared using an ultrasonic cell homogenizer, and then the DNA was subjected to agarose gel analysis to determine the optimal ultrasonic conditions (Fig. 6a).

After shearing, supernatant lysate was added to a new EP tube, and anti-H3K4me3 (4 μl) and H3K27me3 (4 μl) were added and then rotated at 4 °C overnight. Sixty-microliter protein G agar-beads were then added to each immunoprecipitation reaction to precipitate the target fragment. ChIP DNA was purified and quantified using real-time PCR with SYBR Green Supermix. To calculate the relative fold change, the $2^{-\Delta\Delta Ct(\text{normalized ChIP})}$ cycle threshold method was used to determine the levels of H3K27me3 and H3K4me3 around the promoters of signature genes Zbtb16 and Tbx21. The following primer sequences were used:

Zbtb16, forwrd, 5′-AGCCCTTGCCTGTACAAAGA-3′
Zbtb16, reverse, 5′-TGCCTCACCAACCTTTCTTC-3′
Tbx21, forwrd, 5′-TGAAACTTCACTGGAGCGGG-3′
Tbx21, reverse, 5′-TTCATAAAGCCACAGCAAAGGC-3′

Statistical analysis

Data were presented as mean ± standard error or standard deviation. All samples represent independent experiments with biological replicates. One-way ANOVA with post multiple comparisons was applied as indicated. $P < 0.05$ was considered statistically significant. All statistical analyses for animal studies were calculated using SPSS 24.0 software.

Results

Establishment of the mouse RA model

hGPI325-339 and hGPI469-483 were used to establish the mouse RA model. We determined successful RA model establishment by monitoring mouse body weight changes, arthritis index score, joint redness and swelling, foot and ankle arthritis inflammatory cell infiltration, and mouse serum cytokine levels. The success rate of the modeling was 93% (Chen et al. 2019).

Significant reduction of peripheral blood iNKT cells in RA mice

The rates of iNKT cells in the peripheral blood of RA model mice were significantly decreased ($P < 0.05$) and were the lowest at day 14 ($P < 0.05$). The rates of iNKT cells in the peripheral blood increased significantly during the remission phase ($P < 0.05$) compared to the progressive phase (day 11) and the peak phase (day 14) (Figs. 1a and 2a).

The rates of thymus and spleen iNKT cells and the absolute number of thymus iNKT cells in RA mice were significantly decreased

The rates of thymus and spleen iNKT cells and the absolute number of thymus iNKT cells in RA mice were significantly decreased ($P < 0.05$) and were the lowest during the peak of inflammation (day 14). The rates and number of iNKT cells during the remission phase were significantly higher compared to those in the progressive (day 11) and peak phases (day 14) ($P < 0.05$) (Figs. 1b, c and 2b–d).

The proportion of iNKT cell subsets in the thymus and spleen of RA mice were atypical

RA mice had significantly increased proportion of iNKT1 in the thymus and spleen during the progressive (day 11)

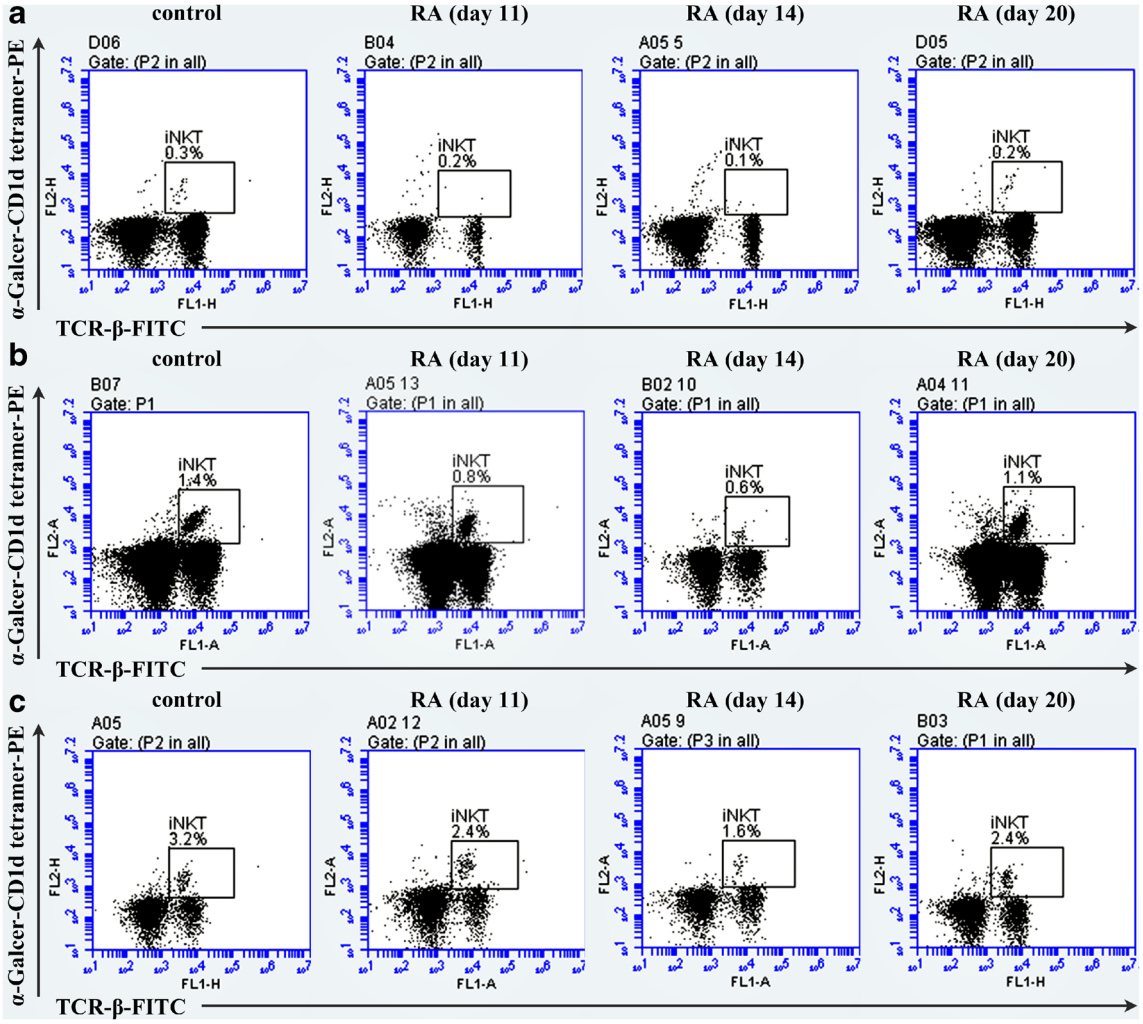

Fig. 1 Flow diagram depicting the rates of iNKT. **a** Peripheral blood. **b** Thymus. **c** Spleen

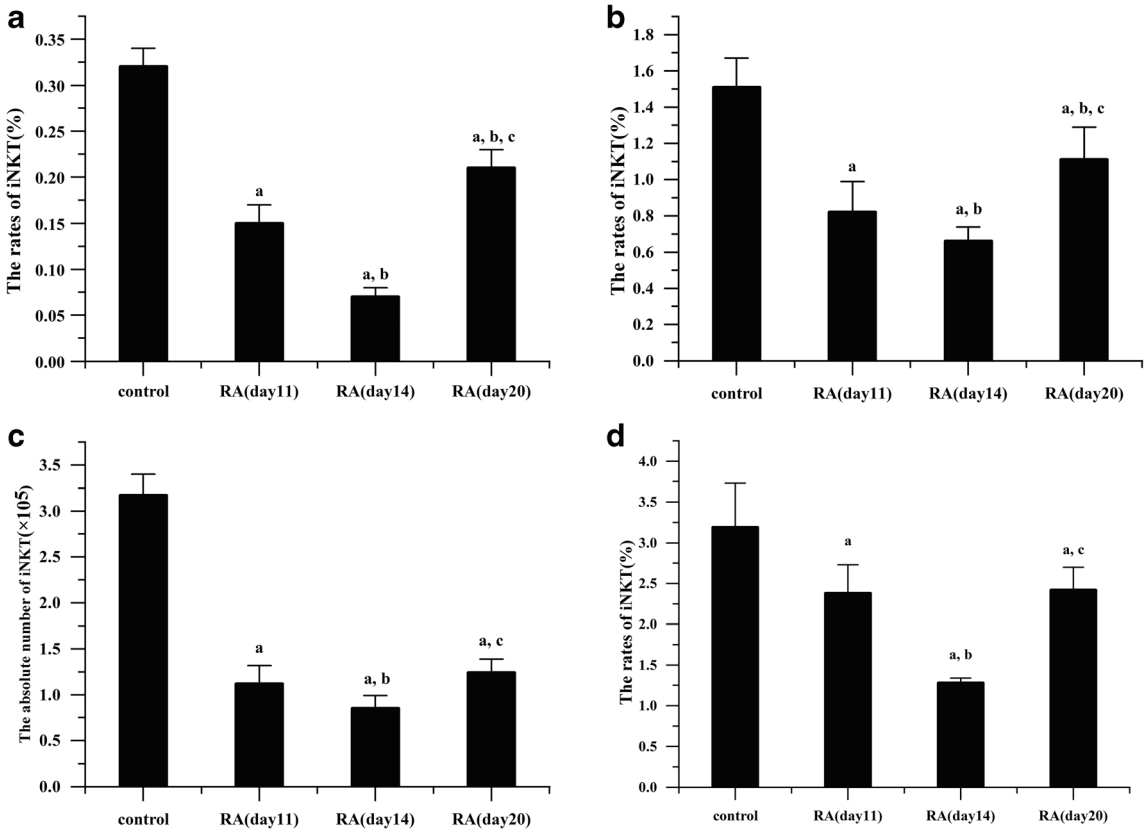

Fig. 2 The rates and absolute number of iNKT cells in RA mice were significantly reduced. [a]$P < 0.05$ vs control; [b]$P < 0.05$ vs RA (day 11); [c]$P < 0.05$ vs RA (day 14). **a** The rates of iNKT in the peripheral blood. **b** The rates of iNKT in the thymus. **c** The absolute number of iNKT in the thymus. **d** The rates of iNKT in the spleen

and peak phases (day 14) ($P < 0.05$), peaking at day 14. The proportion of iNKT2 cells were significantly decreased during the progression phase (day 11) ($P < 0.05$) and were significantly increased during the peak phase (day 14) ($P < 0.05$). The proportion of iNKT17 was significantly increased during the progression phase (day 11) ($P < 0.05$) and was significantly decreased ($P < 0.05$) at peak phase (day 14). Compared to the controls, iNKT1/iNKT2 ratios in the RA model group were increased significantly at all stages ($P < 0.05$) and reached a maximum at peak inflammation before reducing (Figs. 3 and 4).

Expression of PLZF was down-regulated in DP T cells of RA mice, while the expression of T-bet was increased in iNKT cells

During progressive (day 11) and the peak phase (day 14), PLZF protein expression in thymus DP T cells of RA model mice was significantly downregulated ($P < 0.05$), while T-bet protein expression in thymus iNKT cells was significantly upregulated ($P < 0.05$). Compared to the progressive stage (day 11), there were no significant differences in PLZF protein expression levels in thymus DP T cells of RA model mice ($P > 0.05$) during the peak phase (day 14), while thymus iNKT T-bet amounts remained elevated ($P < 0.05$) (Fig. 5).

PLZF mRNA expression was down-regulated in DP T cells of RA mice, while T-bet mRNA expression was increased in iNKT cells

During the progressive (day 11) and peak phases (day 14), PLZF mRNA levels in thymus DP T cells of RA model mice were significantly downregulated ($P < 0.05$), while T-bet mRNA levels in thymus iNKT cells were significantly upregulated ($P < 0.05$). Compared to the progressive phase (day 11), PLZF mRNA expression in thymus DP T cells was significantly decreased, while T-bet mRNA expression in thymus iNKT cells was significantly increased in the peak phase (day 14) ($P < 0.05$) (Fig. 5).

H3K27me3 in the promoter region of Zbtb16 gene in thymus DP T cells of RA mice was significantly increased, while no significant changes in H3K4me3 were observed

H3K27me3 levels in the promoter region of Zbtb16 gene in thymus DP T cells of RA mice were significantly increased in

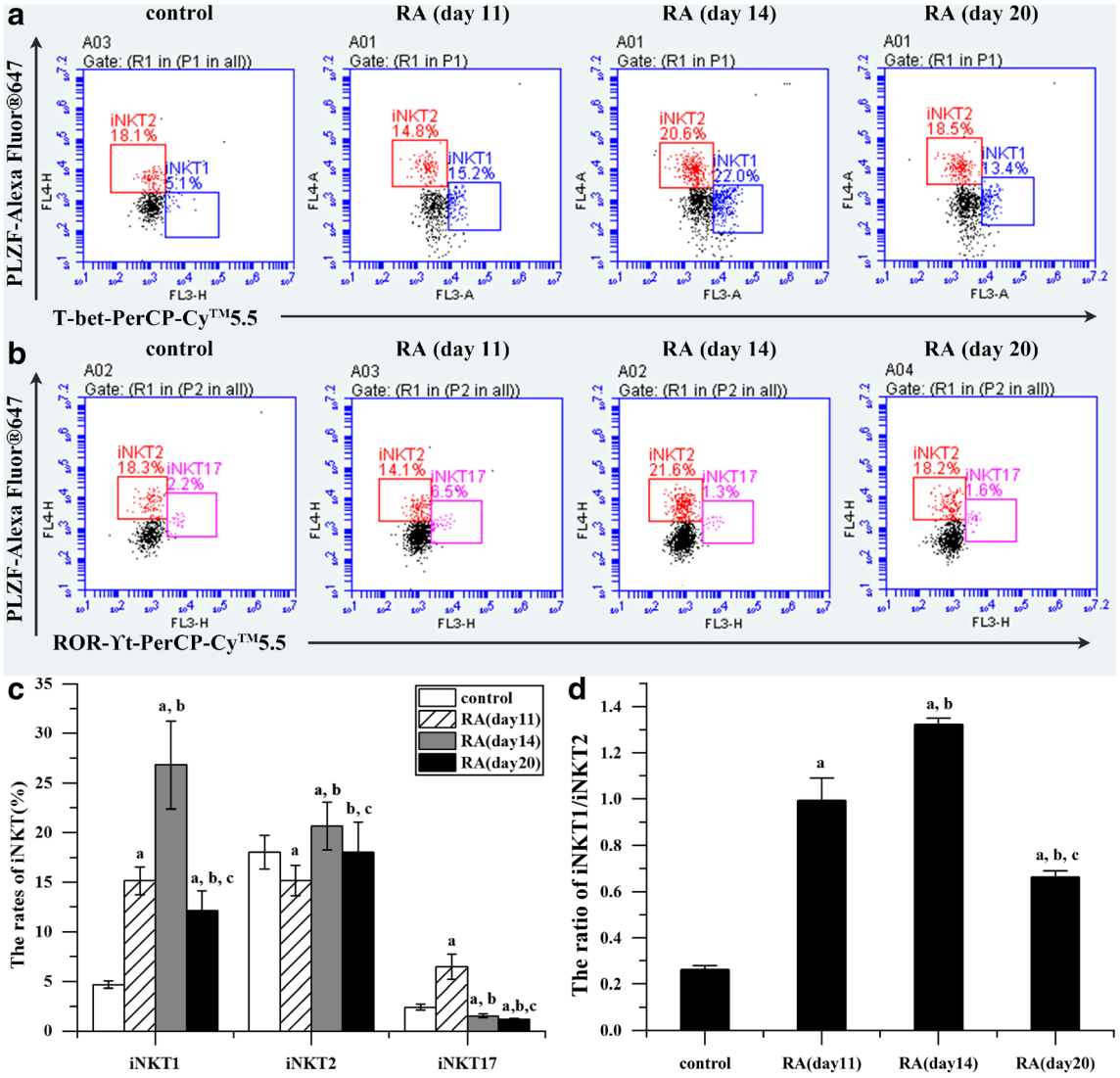

Fig. 3 The proportion of iNKT subsets in the thymus of RA mice was atypical. [a]$P < 0.05$ vs control; [b]$P < 0.05$ vs RA (day 11); [c]$P < 0.05$ vs RA (day 14). **a**, **b** Flow diagram of iNKT1, iNKT2, and iNKT17 in the thymus. **c** The proportion of iNKT1 and iNKT17 increased significantly, while the proportion of iNKT2 decreased significantly. **d** The ratio of iNKT1/iNKT2 was increased significantly in the thymus

both the progressive (day 11) and peak phase (day 14) of inflammation ($P < 0.05$). At the peak phase of inflammation (day 14), H3K27me3 levels were significantly higher compared to the progressive phase (day 11) ($P < 0.05$). There was no significant difference in H3K4me3 levels in the promoter region of Zbtb16 gene in thymus DP T cells of mice for all the groups (Fig. 6b).

H3K4me3 levels in the Tbx21 gene promoter region of thymocyte iNKT cells in RA mice were significantly increased, while H3K27me3 levels were unchanged

We found that there was no significant difference in H3K27me3 levels in the promoter region of Tbx21 gene in thymus iNKT cells of mice in all the groups. H3K4me3 levels in the promoter region of Tbx21 gene in thymus iNKT cells of RA mice were significantly increased in both the progressive (day 11) and peak phase (day 14) of inflammation ($P < 0.05$). At the peak phase of inflammation (day 14), H3K4me3 levels were significantly higher compared to the progressive phase (day 11) ($P < 0.05$) (Fig. 6c).

Expression of UTX in thymic lymphocytes of RA mice was significantly decreased

UTX protein levels in the thymus of RA model mice were significantly downregulated ($P < 0.05$) at the progressive (day 11) and peak phases (day 14). Compared to the progressive phase (day 11), UTX protein levels were lower at peak phase (day 14) of inflammation ($P < 0.05$) (Fig. 5).

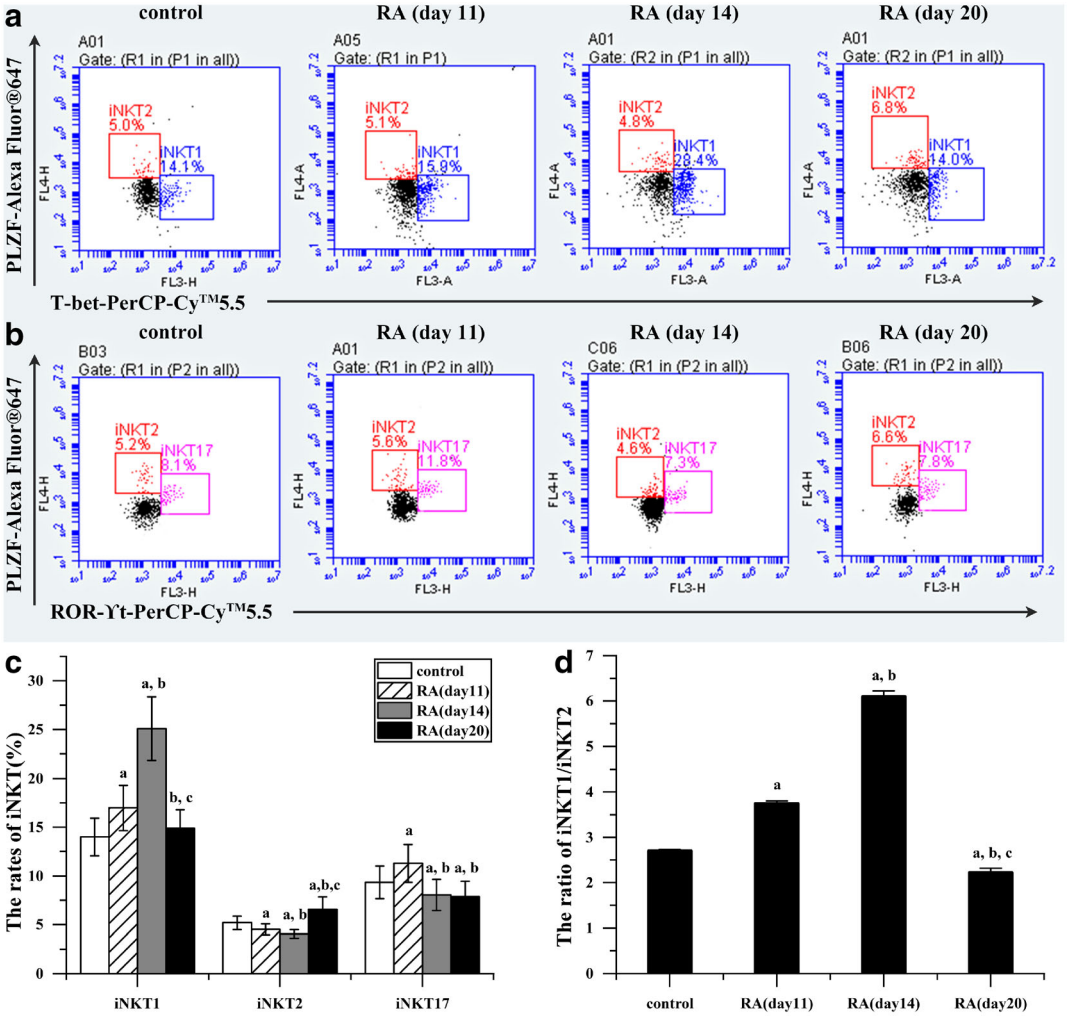

Fig. 4 The proportion of iNKT subsets in the spleen of RA mice was atypical. $^{a}P < 0.05$ vs control; $^{b}P < 0.05$ vs RA (day 11); $^{c}P < 0.05$ vs RA (day 14). **a**, **b** Flow diagram of iNKT1, iNKT2, and iNKT17 in the spleen. **c** The proportion of iNKT1 and iNKT17 increased significantly, while the proportion of iNKT2 decreased significantly. **d** The ratio of iNKT1/iNKT2 was increased significantly in the spleen

Discussion

Glucose-6-phosphoisomerase (GPI) is a frequently used indicator for clinical diagnosis and activity measurement of RA. Recombinant human GPI antigen can induce joint inflammation in mice similar to RA observed in humans (Schubert et al. 2004). In terms of dependence on $CD4^{+}$T cells and reactivity to biological agents, GPI-induced arthritis is closer to the characteristics of human RA (Horikoshi et al. 2012). In our laboratory, modified GPI was used to construct an RA mouse model. Based on the changes in body weight, arthritis index score, foot pad thickness, foot and ankle arthritis cell infiltration, and serum cytokine levels, mice were divided into the progressive phase of inflammation (11 days after modeling), the peak phase (14 days after modeling), and the regressive phase (20 days after modeling) (Chen et al. 2019).

The majority of iNKT cells are differentiated by $CD4^{+}CD8^{+}$(DP) T cells in the thymus (Dashtsoodol et al. 2017; Gapin 2016). The earliest transcription factors that are observed during differentiation are the early growth response transcription factor 2 (egr-2), the E protein family (E2A, HEB), and the zinc finger protein of promyelocytic leukemia (PLZF). PLZF is a necessary transcription factor that regulates the differentiation and development of iNKT cells (Seiler et al. 2012; Savage et al. 2008). In the thymus, iNKT cells undergo stage 0, stage 1, stage 2, and stage 3, and finally differentiate into three major subgroups: iNKT1 (expressing T-bet), iNKT2 (high expression of GATA-3 and PLZF), and iNKT17 (expression of PLZF and ROR-ϒt) (Kwon and Lee 2017). Transcription factor T-bet is crucial for the terminal maturation of iNKT cells (Yue et al. 2011; Schubert et al. 2004).

By observing the different stages of inflammation in RA model mice, it was found that the rates of peripheral blood, thymus, and spleen iNKT cells in RA mice were significantly lower compared to healthy control mice. The inflammatory peak was more significant, with an increase in the remissive

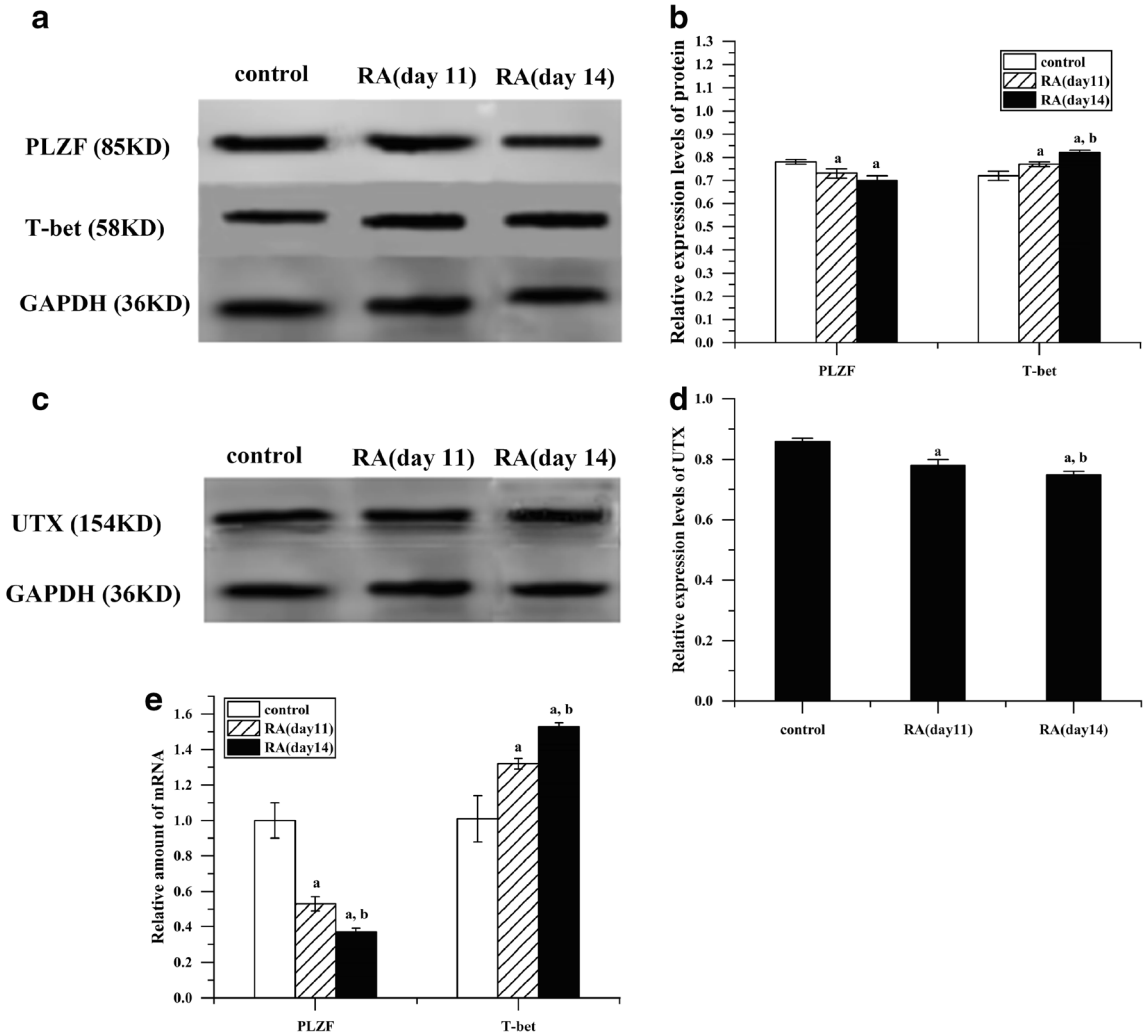

Fig. 5 Expression of PLZF and PLZF mRNA levels was down-regulated in DP T cells of RA mice, while T-bet and T-bet mRNA levels were increased in iNKT cells. [a]$P < 0.05$ vs control; [b]$P < 0.05$ vs RA (day 11); [c]$P < 0.05$ vs RA (day 14). **a**, **b** Relative expression levels of PLZF in DP T cells and T-bet in iNKT cells. **c**, **d** Relative expression levels of UTX in thymic lymphocytes. **e** Relative expression levels of PLZF mRNA in DP T cells and T-bet mRNA in iNKT cells

period. Subgroup analysis of thymus and spleen iNKT cells showed that iNKT1 cells and the ratio of iNKT1/iNKT2 were significantly increased in the progressive, peak, and remission stages of inflammation, and was highest at the peak of inflammation. The rates of iNKT2 cells significantly decreased during the progression of inflammation but increased significantly at the peak phase of inflammation, and returned to normal levels during the remission of inflammation. iNKT17 was highest in the progression of inflammation and significantly decreased at the peak and the remission phase. These results suggest that the iNKT subpopulation of the mouse thymus is imbalanced during the pathogenesis of RA. The increase in iNKT1 and iNKT17 subpopulations is mainly induced by the release of inflammatory cytokines IFN-ϒ and IL-17A and may be involved in the occurrence of RA. Since the number of iNKT1 cells increased significantly in both the progression and peak periods of inflammation, while iNKT17 proportion increased only during the progression stage, we believe that iNKT1 may play a more important role in the occurrence and development of RA. iNKT2 (mainly responsible for the release of anti-inflammatory cytokine IL-4) decreased significantly in the progressive phase of inflammation but increased during the peak phase. We speculated that the increase in iNKT2 may be due to the feedback effect of peripheral inflammation in the thymus, which may play an important role in the recovery of inflammation.

We found that PLZF protein and mRNA levels were significantly reduced in thymus DP T cells, while T-bet protein and mRNA in iNKT cells were significantly increased at the stage of inflammation progression and at the peak of inflammation. This suggests that the decrease in PLZF levels may be an important reason for the decrease in the rates of iNKT cells

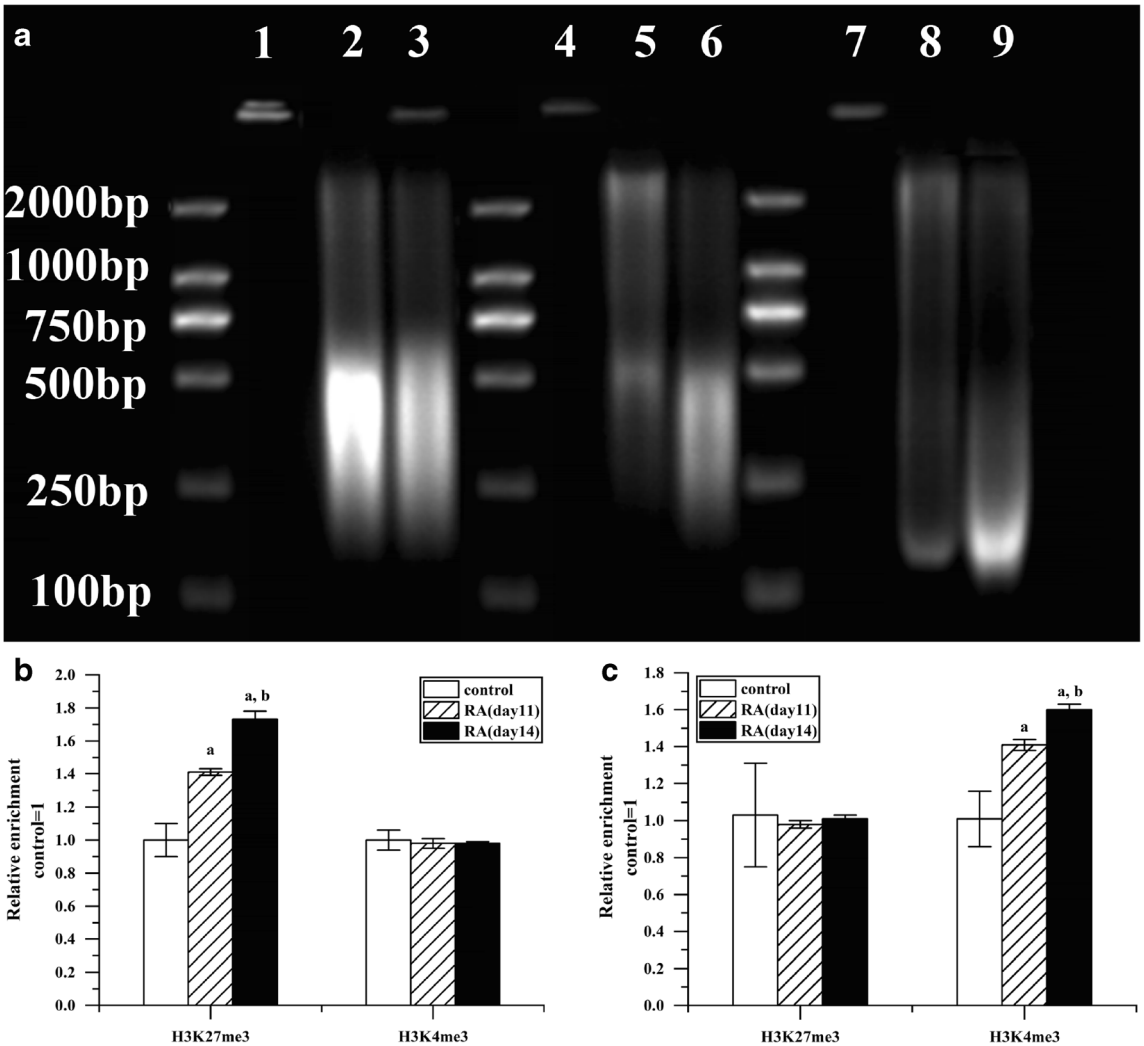

Fig. 6 Histone H3K27me3 and H3K4me3 modification levels in Zbtb16 and Tbx21 gene promoter regions. $^{a}P < 0.05$ vs control; $^{b}P < 0.05$ vs RA (day 11); $^{c}P < 0.05$ vs RA (day 14). **a** Schematic diagram of purified DNA gel electrophoresis after cell sonication. Lanes 1, 4, and 7: pre-ultrasonic crushing; lane 2: 10^7/ml, 20%, 10 s/60 s, 2 times; lane 3: 10^7/ml, 20%, 10 s/60 s, 3 times; lane 5: 5×10^6/ml, 20%, 10 s/60 s, 2 times; lane 6: 5×10^6/ml, 20%, 10 s/60 s, 3 times; lane 7: 2.5×10^6/ml, 20%, 10 s/60 s, 2 times; lane 8: 2.5×10^6/ml, 20%, 10 s/60 s, 3 times. **b** Histone methylation in the promoter region of Zbtb16. **c** Histone methylation in the promoter region of Tbx21

in the thymus and peripheral blood. The increase of T-bet is closely associated with the increase of iNKT1 in the thymus.

Recent studies have found that the promoter regions of Zbtb16 and Tbx21 genes are modified by H3K27me3 and H3K4me3, and are associated with the transcriptional inhibition and activation of genes, respectively (Beyaz et al. 2016). We observed that H3K27me3 levels in the promoter region of Zbtb16 gene were increased, while H3K4me3 levels in the promoter region of Tbx21 gene were increased. Hence, we concluded that the increase in H3K27me3 levels in the promoter region of Zbtb16 resulted from the decrease in PLZF levels, which in turn resulted in the decreased rates of peripheral blood and thymic iNKT cells in RA mice. In addition, higher H3K4me3 levels in the promoter region of Tbx21 resulted in increased T-bet, which consequently resulted in the increased proportion of iNKT1 cells in the thymus of RA mice.

Histone methylation is a reversible process regulated by histone methyltransferase and demethylase. Histone demethylase UTX can promote target gene transcription by removing H3K27me2/3 methyl. UTX is a member of the H3K4 methyltransferase complex MLL2, which promotes gene transcription by regulating H3K4 methylation. Daniel Northrup et al. found that key transcription factors (PLZF, T-bet) for iNKT cell development and differentiation are regulated by UTX (Northrup et al. 2017; Krovi and Gapin 2017). We hypothesized that the elevated levels of H3K27me2/3 during the pathogenesis of RA may be associated with abnormal expression of UTX. To determine this, we measured UTX expression levels in

mouse thymocytes. Our study showed that UTX expression decreased significantly in both the progressive and peak phase of inflammation. This indicated that the increased H3K27me3 modification levels in the promoter region of Zbtb16 gene were associated with the reduced UTX expression of histone demethylase.

In summary, we investigated the epigenetic mechanism that affected the number and abnormal differentiation of iNKT cells in an RA mouse model through H3K27me3 and H3K4me3 modification levels. These results may provide new understanding to the pathogenesis of RA and may be helpful for identifying potential intervention targets for the treatment of RA.

Acknowledgments This work was supported by the National Natural Science Foundation of China (NSFC) (81771755), Colleges and University's Science and Technology Key Research Project of Hebei Province (ZD2017009), the Animal Lab of Medical Experiment Center of Hebei University, and Key Laboratory of Pathogenesis mechanism and control of inflammatory-autoimmune diseases in Hebei Province.

Compliance with ethical standards

All experiments were approved by the Animal Welfare and Ethical Committee of Hebei University (approval number IACUC-2017009).

Conflict of interest The authors declare that they have no conflict of interest.

References

Bartova E, Krejci J, Harnicarova A et al (2008) Histone modifications and nuclear architecture: a review. J Histochem Cytochem 56:711–721. https://doi.org/10.1369/jhc.2008.951251

Beyaz S, Kim JH, Pinello L, Xifaras ME, Hu Y, Huang J, Kerenyi MA, Das PP, Barnitz RA, Herault A, Dogum R, Haining WN, Yilmaz ÖH, Passegue E, Yuan GC, Orkin SH, Winau F (2016) The histone demethylase UTX regulates the lineage-specific epigenetic program of invariant natural killer t cells. Nat Immunol 18:184–195. https://doi.org/10.1038/ni.3644

Boissier MC, Assier E, Falgarone G, Bessis N (2008) Shifting the imbalance from th1/th2 to th17/treg: the changing rheumatoid arthritis paradigm. Joint Bone Spine 75:373–375. https://doi.org/10.1016/j.jbspin.2008.04.005

Chen D, Liu H, Wang Y, Chen S, Liu J, Li W, Dou H, Hou W, Meng M (2019) Study of the adoptive immunotherapy on rheumatoid arthritis with Thymusderived invariant natural killer T cells. Int Immunopharmacol 67:427–440. https://doi.org/10.1016/j.intimp.2018.12.040

Cho YW, Hong T, Hong S, Guo H, Yu H, Kim D, Guszczynski T, Dressler GR, Copeland TD, Kalkum M, Ge K (2007) Ptip associates with mll3- and mll4-containing histone h3 lysine 4 methyltransferase complex. J Biol Chem 282:20395–20406. https://doi.org/10.1074/jbc.M701574200

Couture JF, Trievel RC (2006) Histone-modifying enzymes encryptingan enigmatic epigeneti code. Curropin Struct Biol 16:753–760. https://doi.org/10.1016/j.sbi.2006.10.002

Dashtsoodol N, Shigeura T, Aihara M (2017) Alternative pathway for the development of Va14+NKT cells directly from CD4-CD8-thymocytes that bypasses the CD4+CD8+stage. Nat Immunol 18:274–284. https://doi.org/10.1038/ni.3668

Gapin, & Laurent. (2016). Development of invariant natural killer t cells. Curr Opin Immunol, 39, 68-74. https://doi.org/10.1016/j.coi.2016.01.001

Horikoshi M, Goto D, Segawa S, Yoshiga Y, Iwanami K, Inoue A, Tanaka Y, Matsumoto I, Sumida T (2012) Activation of invariant nkt cells with glycolipid ligand α-galactosylceramide ameliorates glucose-6-phosphate isomerase peptide-induced arthritis. PLoS One 7:e51215. https://doi.org/10.1371/journal.pone.0051215

Issaeva I, Zonis Y, Rozovskaia T, Orlovsky K, Croce CM, Nakamura T, Mazo A, Eisenbach L, Canaani E (2007) Knockdown of alr (mll2) reveals alr target genes and leads to alterations in cell adhesion and growth. Mol Cell Biol 27:1889–1903. https://doi.org/10.1128/MCB.01506-06

Krovi SH, Gapin L (2017) iNKT cells need UTX-TRA demethylation. Nat Immunol 18:148–150. https://doi.org/10.1038/ni.3663

Kwon DI, Lee YJ (2017) Lineage differentiation program of invariant natural killer T cells. Immune Network 17:365–377. https://doi.org/10.4110/in.2017.17.6.365

Matsuda JL, Zhang Q, Ndonye R et al (2006) T-bet concomitantly controls migration, survival and effector functions during the development of v 14i NKT cells. Blood 107:2797–2805. https://doi.org/10.1182/blood-2005-08-3103

Meng M, Chen D, Xu M et al (2015) Study of the correlation between the percentage of iNKT cells and the ratio of IFN-γ/IL-4 in patients with rheumatoid arthritis. Microbiol Immunol 6:423–429. https://doi.org/10.3892/ol.2017.7484

Ng SS, Yue WW, Oppermann U, Klose RJ (2009) Dynamic protein methylation in chromatin biology. Cell Mol Life Sci (CMLS) 66:407–422. https://doi.org/10.1007/s00018-008-8303-z

Northrup D, Yagi R, Cui K, Proctor WR, Wang C, Placek K, Pohl LR, Wang R, Ge K, Zhu J, Zhao K (2017) Histone demethylases UTX and jmjd3 are required for NKT cell development in mice. Cell Biosci 7:25–39. https://doi.org/10.1186/s13578-017-0152-8

Savage AK, Constantinides MG, Han J, Picard D, Martin E, Li B, Lantz O, Bendelac A (2008) The transcription factor PLZF directs the effector program of the NKT cell lineage. Immunity 29:391–403. https://doi.org/10.1016/j.immuni.2008.07.011

Schubert D, Maier B, Morawietz L, Krenn V, Kamradt T (2004) Immunization with glucose-6-phosphate isomerase induces T cell-dependent peripheral polyarthritis in genetically unaltered mice. J Immunol 172:4503–4509. https://doi.org/10.4049/jimmunol.172.7.4503

Seiler MP, Mathew R, Liszewski MK, Spooner CJ, Barr K, Meng F, Singh H, Bendelac A (2012) Elevated and sustained expression of the transcription factors egr1 and egr2 controls NKT lineage differentiation in response to TCR signaling. Nat Immunol 13:264–271. https://doi.org/10.1038/ni.2230

Tudhope SJ, Delwig AV, Falconer J et al (2010) Profound invariant natural killer T-cell deficiency in inflammatory arthritis. Ann Rheum Dis 69:1873–1879. https://doi.org/10.1136/ard.2009.125849

Véronique P, Chifflot H, Sibilia J, Muller S, Monneaux F (2010) Rituximab treatment overcomes reduction of regulatory iNKT cells in patients with rheumatoid arthritis. Clin Immunol 134:331–339. https://doi.org/10.1016/j.clim.2009.11.007

Wang D, Xia X, Weiss RE, Refetoff S, Yen PM (2010) Distinct and histone-specific modifications mediate positive versus negative transcriptional regulation of tshα promoter. PLoS One 5:e9853. https://doi.org/10.1371/journal.pone.0009853

Yi L, Li Z, Hu T, Liu J, Li N, Cao X, Liu S (2019) Intracellular HSP70L1 inhibits human dendritic cell maturation by promoting suppressive H3K27me3 and H2AK119Ub1 histone modifications. Cell Mol Immunol 11:1–10. https://doi.org/10.1038/s41423-018-0195-8

Yue X, Izcue A, Borggrefe T et al (2011) Essential role of mediator subunit med1 in invariant natural killer T-cell development. Proc

Natl Acad Sci 108:17105–17110. https://doi.org/10.1073/pnas.1109095108

Zhang Q, Long H, Liao J et al (2011) Inhibited expression of hematopoietic progenitor kinase 1 associated with loss of jumonji domain containing 3 promoter binding contributes to autoimmunity in systemic lupus erythematosus. J Autoimmun 37:180–189. https://doi.org/10.1016/j.jaut.2011.09.006

Zhang X, Liu J, Yang F et al (2016) Immunization with mixed peptides derived from glucose-6-phosphate isomerase induces rheumatoid arthritis in DBA/1 mice. Chin J Pathophysiol 32:569–576. https://doi.org/10.3969/j.issn.1000-4718.2016.03.031